PHENIX results on elliptic and triangular flow from the small-system geometry scan at 200 GeV

doi: 10.1016/j.nuclphysa.2018.09.050

Available online at www.sciencedirect.com

ScienceDirect

Nuclear Physics A 982 (2019) 471–474

www.elsevier.com/locate/nuclphysa

XXVIIth International Conference on Ultrarelativistic Nucleus-Nucleus Collisions (Quark Matter 2018)

PHENIX results on elliptic and triangular flow from the small-system geometry scan at 200 GeV

Sylvia Morrow for the PHENIX Collaboration

Department of Physics and Astronomy, Vanderbilt University, Nashville, TN 37235, USA

Abstract

Using the extraordinary versatility of RHIC in selecting different colliding species, the PHENIX experiment has collected data in p+Al, p+Au, d+Au, and ^{3}He+Au collisions at 200 GeV center-of-mass energy and conducted a comprehensive set of anisotropic flow measurements. These geometry-controlled experiments provide a unique testing ground for theoretical models that produce azimuthal particle correlations based on initial- and/or final-state effects.

A complete set of triangular anisotropies of inclusive charged particles and final results on identified pion and proton $v_2(p_T)$ are shown. The mass-ordered splitting in $v_2(p_T)$ provides information about the role of early-stage collective flow and late-stage hadronic rescattering. Detailed model comparisons with all observables are discussed.

Keywords: quark gluon plasma, collective flow, small systems

1. Introduction

Azimuthal correlations in small collision systems (p+p and p+A) test the applicability of models of quark-gluon plasma (QGP) in situations where regions of matter which exceed the critical energy density for QGP formation are extremely small, short-lived, and may not reach thermal equilibrium. Anisotropic azimuthal distributions have been considered characteristic of the presence of a strongly coupled medium, but alternative model formalisms such as parton transport and initial-state momentum correlations produce azimuthally correlated distributions in these systems that emerge without the presence of QGP. RHIC's small system geometry scan – $p/d/^3$He+Au collisions at $\sqrt{s_{NN}}$ = 200 GeV – provides unique discrimination between these proposed explanations of the origin of azimuthal anisotropy in small systems.

Previous PHENIX analyses extracted charged hadron $v_2(p_T)$ in all three aforementioned collision systems and $v_3(p_T)$ in ^{3}He+Au [1, 2, 3]. New PHENIX analyses complement this set of results with $v_3(p_T)$ in p/d+Au [4] and $v_2(p_T)$ for identified pions and protons in all three systems [5].

2. Experiment

This work uses the event plane method to extract the v_n coefficients to the Fourier decomposition of $dN/d\phi$, with $n = 2$ and $n = 3$ quantifying ellipticity and triangularity, respectively. That is,

https://doi.org/10.1016/j.nuclphysa.2018.09.050

$v_n(p_T) = \langle\cos(n(\phi_{\text{particle}}(p_T) - \Psi_n^{\text{EPdetector}}))\rangle/\text{Res}(\Psi_n^{\text{EPdetector}})$, where ϕ_{particle} is the azimuthal angle of the reconstructed track measured at midrapidity in the central arms (CNT) of the PHENIX experiment with $|\eta| < 0.35$ [6] and $\Psi_n^{\text{EPdetector}}$ is the event plane angle determined from azimuthal particle distributions at backward rapidity (Au-going direction) [7]. The event plane detectors used in this analysis are the forward silicon vertex detector (FVTX) with $1 < |\eta| < 3$ and the beam-beam counter (BBC) with $3.1 < |\eta| < 3.9$ [8, 9]. The 3-sub event method is used to extract the event plane resolution, $\text{Res}(\Psi_n^{\text{EPdetector}})$, using event plane angles measured by the CNT, FVTX, and BBC.

This analysis uses the 5% most central collision events. For these data sets, PHENIX utilized an online high multiplicity trigger in addition to the minimum bias trigger. Systematic uncertainties applied account for detector misalignment, nonflow contributions, and selection cuts. Nonflow contributions, the largest source of uncertainty particularly at high p_T, have been estimated by comparing to a $p + p$ reference at the same collision energy.

3. Results

In the presence of a common velocity field, measurements of $v_n(p_T)$ with identified hadrons display an ordering determined by the particle mass. Fig. 1 shows measurements of pion and proton $v_2(p_T)$ in $p/d/^3$He+Au collisions. At low p_T (below $p_T \approx 1.5$ GeV/c) the pion v_2 in each system is measured to be larger than the proton v_2 and at high p_T (above $p_T \approx 1.5$ GeV/c) this trend reverses (more visually apparent in Fig. 3). Calculations from the hydrodynamical model iEBE-VISHNU in Fig. 1 show significant

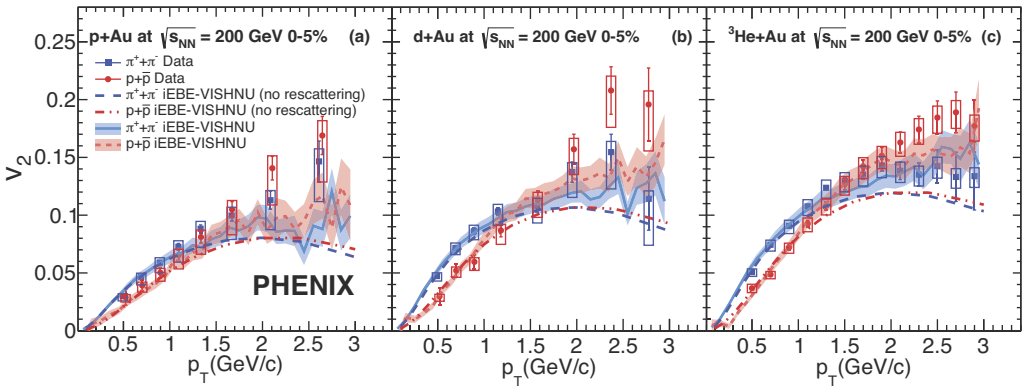

Fig. 1. Measurements of $v_2(p_T)$ for identified pions and protons in (a) p+Au, (b) d+Au, and (c) ^{3}He+Au collisions compared to hydrodynamical model iEBE-VISHNU with and without hadronic rescattering. Error bars represent the statistical uncertainties and boxes are systematic uncertainties.

differences between pion and proton v_2 at low p_T but not at high p_T, regardless of the presence of a hadronic rescattering phase. In contrast, the parton transport model AMPT in Fig. 2 produces significant mass splitting at all p_T unless the hadronic rescattering phase is skipped. Without the hadronic scattering phase, the AMPT simulations predict similar values for pion and proton v_2 at low p_T. This suggests this phase is critical to the formation of mass splitting below $p_T \approx 1$ GeV/c. On the other hand, the mass splitting at high p_T develops in AMPT regardless of the presence of hadronic rescattering. This suggests that this feature emerges in the hadronization phase through quark recombination in contrast to hydrodynamical models which hadronize using a statistical model, Cooper-Frye. It should be noted that while AMPT qualitatively describes the mass ordering features observed in the data, it has yet to be determined if it can describe small and large systems simultaneously.

These same conclusions can be drawn from a ratio of pion v_2 over proton v_2 as shown in Fig. 3. In the ratio some correlated sources of uncertainty partially cancel. The slope of the two hydrodynamical models

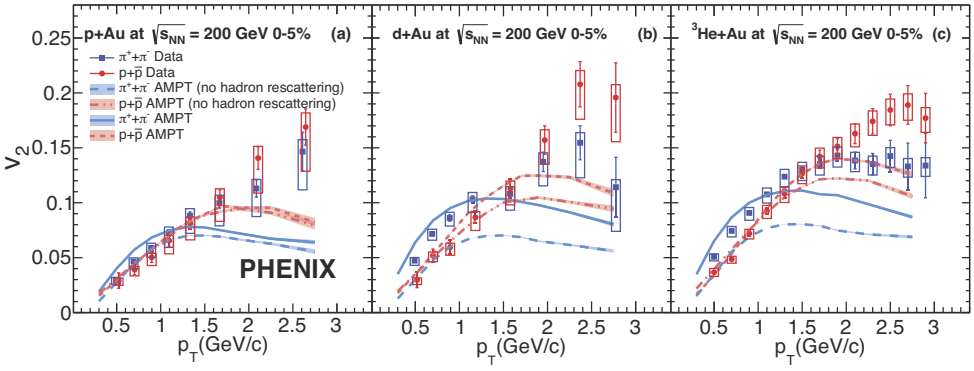

Fig. 2. Measurements of $v_2(p_T)$ for identified pions and protons in (a) p+Au, (b) d+Au, and (c) ^{3}He+Au collisions compared to AMPT with and without hadronic rescattering.

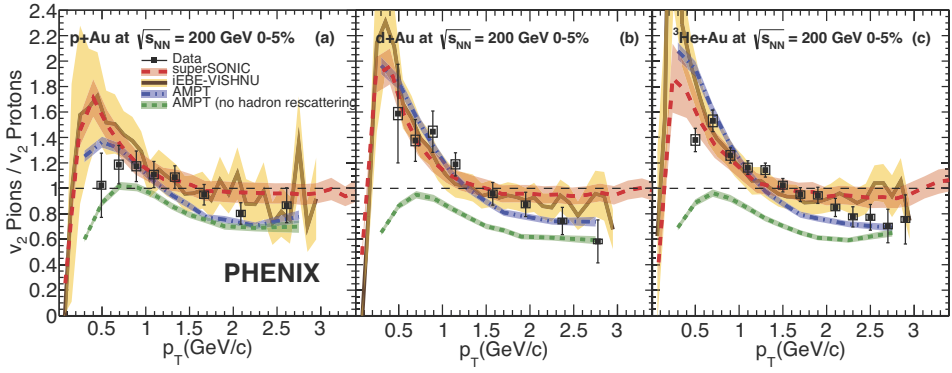

Fig. 3. Measurements of pion v_2 over proton v_2 as a function of p_T in (a) p+Au, (b) d+Au, and (c) ^{3}He+Au collisions compared to superSONIC, iEBE-VISHNU, and AMPT with and without hadronic rescattering.

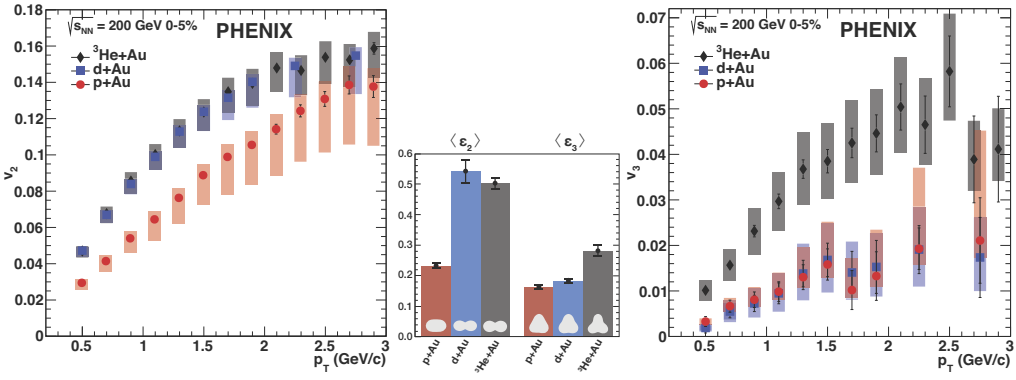

Fig. 4. Measurements of $v_2(p_T)$ (left) and $v_3(p_T)$ (right) in ^{3}He+Au (black diamonds), d+Au (blue squares), p+Au (red circles). Error bars represent the statistical uncertainties and boxes are systematic uncertainties. Average second and third order eccentricity from Glauber Monte Carlo simulations of the initial state for central $p/d/^3$He+Au collisions (center) with statistical uncertainties. Inset shapes illustrate the qualitative degree of ellipticity (ε_2) or triangularity (ε_3).

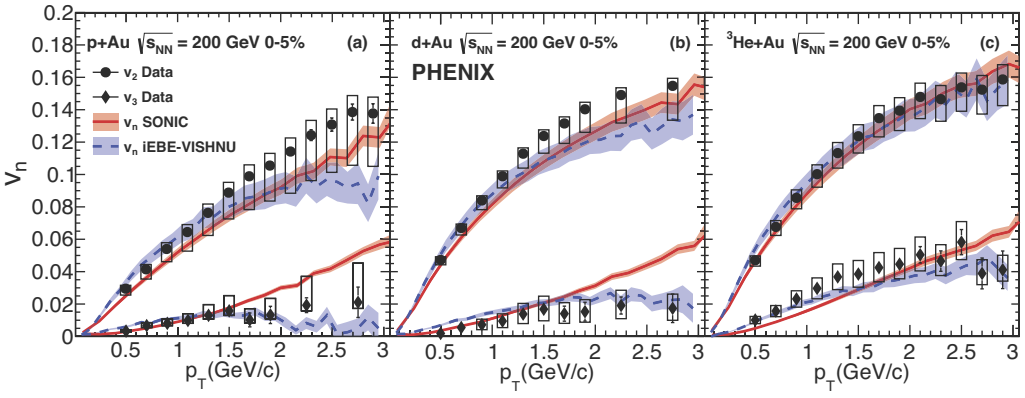

Fig. 5. Measured $v_2(p_T)$ (circles) and $v_3(p_T)$ (diamonds) in (a) p+Au, (b) d+Au, and (c) ^{3}He+Au collisions compared to hydrodynamical model predictions from SONIC (solid red) and iEBE-VISHNU (dashed blue).

(superSONIC and iEBE-VISHNU) agree well with the data at low p_T but the models exhibit no slope at high p_T. The AMPT calculation with a hadronic rescattering phase offers a good description of the measurements while the removal of hadronic rescattering results in a significant discrepancy between the data and theory at low p_T.

The charged hadron $v_n(p_T)$ was measured for $n = 2$ and $n = 3$ for the three collision systems as shown in the left and right panels of Fig. 4. The ordering of these measurements is compared to that of the average initial state eccentricities as calculated by a Monte Carlo Glauber model and shown in the central panel of Fig. 4. The system eccentricities order $\langle\varepsilon_2\rangle_p \approx \langle\varepsilon_2\rangle_d < \langle\varepsilon_2\rangle_{^3He}$ and $\langle\varepsilon_3\rangle_p < \langle\varepsilon_3\rangle_d \approx \langle\varepsilon_3\rangle_{^3He}$ which exactly matches the v_n ordering, $(v_2)_p \approx (v_2)_d < (v_2)_{^3He}$ and $(v_3)_p < (v_3)_d \approx (v_3)_{^3He}$. This result strongly suggests that final-state momentum correlations originate from the spatial distribution of the participating nucleons in the initial state. As shown in Fig. 5, this is consistent with a hydrodynamical picture, and both the SONIC and iEBE-VISHNU calculations are in good agreement with the data.

4. Conclusion

The mass ordering of pion and proton $v_2(p_T)$ measured in p+Au, d+Au and ^{3}He+Au collisions is consistent with the hydrodynamic picture of a velocity field driven by pressure gradients in an initial near-inviscid fluid medium. It is also consistent with AMPT calculations which produce mass ordering primarily through hadronic scattering and quark coalescence. Measurements of charged hadron $v_2(p_T)$ and $v_3(p_T)$ in the three collision systems support the picture of initial-state spatial correlations efficiently translating into final-state momentum correlations. These observations are best described by hydrodynamical models.

References

[1] A. Adare, et al., Phys. Rev. Lett. 115 (14) (2015) 142301. doi:10.1103/PhysRevLett.115.142301.
[2] C. Aidala, et al., Phys. Rev. C 95 (3) (2017) 034910. doi:10.1103/PhysRevC.95.034910.
[3] C. Aidala, et al., Phys. Rev. C 96 (6) (2017) 064905. doi:10.1103/PhysRevC.96.064905.
[4] C. Aidala, et al.arXiv:1805.02973.
[5] A. Adare, et al., Phys. Rev. C 97 (2018) 064904. arXiv:1710.09736, doi:10.1103/PhysRevC.97.064904.
[6] K. Adcox, et al., Nucl. Instrum. Meth. A 499 (2003) 489–507. doi:10.1016/S0168-9002(02)01952-6.
[7] A. M. Poskanzer, S. A. Voloshin, Phys. Rev. C 58 (1998) 1671–1678. doi:10.1103/PhysRevC.58.1671.
[8] C. Aidala, et al., Nucl. Instrum. Methods Phys. Res., Sec. A 755 (2014) 44. doi:10.1016/j.nima.2014.04.017.
[9] M. Allen, et al., Nucl. Instrum. Methods Phys. Res., Sec. A 499 (2003) 549. doi:10.1016/S0168-9002(02)01956-3.